Journal of Sound and Vibration (2001) **243**(1), 43–61
doi:10.1006/jsvi.2000.3391, available online at http://www.idealibrary.com on IDEAL®

IDENTIFICATION OF DAMPING: PART 1, VISCOUS DAMPING

S. ADHIKARI AND J. WOODHOUSE

Department of Engineering, University of Cambridge, Trumpington Street, Cambridge CB2 1PZ, England. E-mail: jw12@eng.ca.mac.uk

(*Received* 4 *May* 2000, *and in final form* 1 *September* 2000)

Characterization of damping forces in a vibrating structure has long been an active area of research in structural dynamics. The most common approach is to use "viscous damping" where the instantaneous generalized velocities are the only relevant state variables that affect damping forces. However, viscous damping is by no means the only damping model within the scope of linear analysis. Any model which makes the energy dissipation functional non-negative is a possible candidate for a valid damping model. This paper, and its companion (see pp. 63–88 of this issue), are devoted to developing methodologies for identification of such general damping models responsible for energy dissipation in a vibrating structure. This paper considers identification of viscous damping under circumstances when the actual damping model in the structure is non-viscous. A method is presented to obtain a full (non-proportional) viscous damping matrix from complex modes and complex natural frequencies. It is assumed that the damping is "small" so that a first order perturbation method is applicable. The proposed method and several related issues are discussed by considering numerical examples based on a linear array of damped spring-mass oscillators. It is shown that the method can predict the spatial location of damping with good accuracy, and also give some indication of the correct mechanism of damping.

1. INTRODUCTION

Characterization of damping forces in a vibrating structure has long been an active area of research in structural dynamics. The demands of modern engineering have led to a steady increase of interest in recent years. However, in spite of a large amount of research, understanding of damping mechanisms is still quite primitive. A major reason for this is that, by contrast with inertia and stiffness forces, it is not in general clear which *state variables* are relevant to determine the damping forces. By far the most common approach is to assume so-called "viscous damping", a linear model in which it is supposed that the instantaneous generalized velocities are the only relevant state variables that determine damping. This approach was first introduced by Rayleigh [1] via his famous "dissipation function", a quadratic expression for the energy dissipation rate with a symmetric matrix of coefficients, the "damping matrix". A further idealization, also pointed out by Rayleigh, is to assume the damping matrix to be a linear combination of the mass and stiffness matrices. Rayleigh was quite clear that this idea was suggested for mathematical convenience only, because it allows the damping matrix to be diagonalized simultaneously with the mass and stiffness matrices, preserving the simplicity of uncoupled, real normal modes as in the undamped case. Since its introduction this model has been used extensively and is now usually known as "Rayleigh damping", "proportional damping" or "classical damping".

0022-460X/01/210043 + 19 $35.00/0

Unfortunately, there is no physical reason why a general system should behave like this. In fact, practical experience in modal testing shows that most real-life structures do not do so, as they possess complex modes instead of real normal modes. As Sestieri and Ibrahim [2] have put it "… it is ironic that the real modes are in fact not real at all, in that in practice they do not exist, while complex modes are those practically identifiable from experimental tests. This implies that real modes are pure abstraction, in contrast with complex modes that are, therefore, the only reality!" However, consideration of complex modes in experimental modal analysis has not been very popular among researchers. In fact, many publications, for example, references [3–5], discuss how to obtain the "best" real normal modes from identified complex modes.

Complex modes will arise with viscous damping, provided it is non-proportional, as Rayleigh himself analyzed in some detail. However, the physical justification for viscous damping is scarcely more convincing than that for Rayleigh damping. Viscous damping is by no means the only damping model within the scope of linear analysis. Any causal model which makes the energy dissipation functional non-negative is a possible candidate for a damping model. In the case of such general linear damping models the question of "proportionality" does not usually arise, and the system will have complex modes. Woodhouse [6] showed that for light damping, such damping models can be handled in a very similar way to viscous models, using a first order perturbation method based on the undamped modes and natural frequencies.

In fact, until this work it was far from clear that the standard procedure of experimental modal analysis actually measured "modes" at all when complex results were obtained. The justification of the method in the standard texts (e.g., Ewins [7]) is based on assuming viscous damping, and begs the question of how one might tell in practice whether a viscous model is applicable to a given structure, let alone of how to proceed if a viscous model is not supported by the measurements. These are the central questions to be addressed in this study. The earlier work (Woodhouse [6]) showed that, provided damping is sufficiently light for first order perturbation theory to be used, then the expression for vibration transfer functions in terms of mode shapes and natural frequencies, familiar from undamped systems, carries over almost unchanged to systems with completely general linear damping. One simply replaces the mode shapes with corresponding complex modes, and the natural frequencies with their corresponding complex values. If the system satisfies reciprocity when driving and observing points are suitably interchanged, then the familiar result carries over exactly. This result shows that experimental modal analysis can indeed measure the correct complex modes of a structure, since the pole-fitting strategy normally used is based on the validity of this transfer function expression. Even if the system is not reciprocal, correct results can be obtained if the observing point is moved over the structure while the driving point is kept fixed (but not if the converse procedure is followed).

There are good arguments to support the principle of reciprocity when the physical mechanism of damping arises from linear viscoelastic behaviour within some or all of the material of which the structure is built. The "correspondence principle" of linear viscoelasticity applies to such problems under rather general conditions (see, e.g., Fung [8]), and since the undamped problem satisfies reciprocity, then the damped one will also do so. However, the case is less obvious for damping associated with structural joints, often the dominant source of damping in practice. The mechanisms of such damping are frequently non-linear when examined in detail, but empirically the overall result frequently satisfies normal experimental tests of linearity. The question of whether such systems should be expected to satisfy reciprocity remains open. For the purpose of the present investigation, reciprocity will be assumed in all cases.

The results based on first order perturbation theory give a firm basis for further analysis, to use the details of the measured complex modes to learn more about the underlying damping mechanisms. There are several general questions of interest:

1. From experimentally determined complex modes can the underlying damping mechanism be identified? Is it viscous or non-viscous? Can the correct model parameters be found experimentally?
2. Is it possible to establish experimentally the *spatial distribution* of damping?
3. Is it possible that more than one damping model with corresponding "correct" sets of parameters may represent the system response equally well, so that the identified model becomes non-unique?
4. Does the selection of damping model matter from an engineering point of view? Which aspects of behaviour are wrongly predicted by an incorrect damping model?

This paper and its companion [9] address these questions. The analysis is restricted to linear systems with light damping: the validity of the first order perturbation results is assumed throughout. The initial aim is to consider what can be learned about these questions in principle, so procedures will be illustrated by applying them to simulated transfer functions, with no noise. The issue of how the usefulness of any procedure might be limited in practice by measurement noise will be deferred to later studies. This paper will concentrate on the fitting of viscous models to "measured" transfer functions, and on establishing the symptoms by which a non-viscous model might be recognized. In section 2, the theory of determination of complex frequencies and modes based on the first order perturbation method are briefly reviewed. In section 3, an algorithm is given for fitting a non-proportional viscous damping model, using the complex modes and complex frequencies. In section 4, numerical examples are given to illustrate the fitting procedure. Some implications of these results for damping identification are summarized in section 5. In the companion paper [9], the procedures are generalized to some non-viscous models of damping, and the discussion extended to this more general case.

2. BACKGROUND OF COMPLEX MODES

The equations of motion for free vibration of a viscously damped linear discrete system with N degrees of freedom can be written as

$$\mathbf{M}\ddot{\mathbf{y}}(t) + \mathbf{C}\dot{\mathbf{y}}(t) + \mathbf{K}\mathbf{y}(t) = \mathbf{0}, \tag{1}$$

where $\mathbf{M}$, $\mathbf{C}$ and $\mathbf{K}$ are $N \times N$ mass, damping and stiffness matrices, respectively, and $\mathbf{y}(t)$ is the $N \times 1$ vector of the generalized co-ordinates. A harmonic solution of the form $\mathbf{y}(t) = \mathbf{z}\exp[\mathrm{i}\lambda t]$ is sought. Substitution of $\mathbf{y}(t)$ in equation (1) yields

$$-\lambda^2\mathbf{M}\mathbf{z} + \mathrm{i}\lambda\mathbf{C}\mathbf{z} + \mathbf{K}\mathbf{z} = \mathbf{0}. \tag{2}$$

This equation is satisfied by the jth latent root (complex natural frequency), λ_j and jth latent vector (mode shape), $\mathbf{z}_j$, of the $\lambda -$ matrix problem (see Lancaster [10]), so that

$$-\lambda_j^2\mathbf{M}\mathbf{z}_j + \mathrm{i}\lambda_j\mathbf{C}\mathbf{z}_j + \mathbf{K}\mathbf{z}_j = \mathbf{0}. \tag{3}$$

Unless $\mathbf{C}$ is simultaneously diagonalizable with $\mathbf{M}$ and $\mathbf{K}$ (conditions for which were derived by Caughey and O'Kelly [11]), in general λ_j and $\mathbf{z}_j$ will be complex. Procedures to obtain the complex eigensolutions follow two main routes: the state-space method and approximate methods in "N-space". The state-space method (see Newland [12]), although exact in nature, requires significant numerical effort for obtaining the eigensolutions as the size of the problem doubles. More significantly, this method also lacks some of the intuitive simplicity of traditional modal analysis. For these reasons there has been considerable research effort to calculate the complex eigensolutions of non-proportionally damped structures in N-space. Using first order perturbation analysis, Rayleigh [1] considered approximate methods to determine λ_j and $\mathbf{z}_j$ by assuming the elements of $\mathbf{C}$ are small but otherwise general. Cronin [13] has given a power series expression for eigenvalues and eigenvectors by using a perturbation method. For later reference, the main results for calculation of complex modes and frequencies using first order perturbation theory are outlined briefly. The undamped natural frequencies ω_j and mode shapes $\mathbf{x}_j$ satisfy

$$\mathbf{K}\mathbf{x}_j = \omega_j^2 \mathbf{M}\mathbf{x}_j \quad \text{for } j = 1, \ldots, N. \tag{4}$$

The mode shape vectors are normalized in usual way so that

$$\mathbf{x}_k^{\mathrm{T}}\mathbf{M}\mathbf{x}_j = \delta_{jk}, \quad \mathbf{x}_k^{\mathrm{T}}\mathbf{K}\mathbf{x}_j = \omega_j^2 \delta_{jk}, \tag{5}$$

where δ_{jk} is the Kroneker delta function and $(\bullet)^{\mathrm{T}}$ denotes matrix transpose. Since $\{\mathbf{x}_j\}$ form a complete set of vectors $\mathbf{z}_j$ can be expanded as a linear combination of $\mathbf{x}_j$. Provided the entries of the $\mathbf{C}$ matrix are all small, the roots of equation (3), λ_j, will be close to those of equation (4), ω_j, and the corresponding eigenvectors, $\mathbf{z}_j$, are also expected to be close to $\mathbf{x}_j$. Thus, a solution can be tried of the form

$$\mathbf{z}_j = \sum_{l=1}^{N} \alpha_l^{(j)} \mathbf{x}_l \quad \text{where } \alpha_j^{(j)} = 1 \quad \text{and} \quad |\alpha_l^{(j)}| \ll 1 \ \ \forall l \neq j. \tag{6}$$

Substituting $\mathbf{z}_j$ into equation (3), premultiplying by $\mathbf{x}_k^{\mathrm{T}}$ and using the orthogonality properties of the undamped mode shapes described by equation (5) yields

$$-\lambda_j^2 \alpha_k^{(j)} + \mathrm{i}\lambda_j \sum_{l=1}^{N} \alpha_l^{(j)} C'_{kl} + \omega_k^2 \alpha_k^{(j)} = 0, \tag{7}$$

where $C'_{kl} = \mathbf{x}_k^{\mathrm{T}}\mathbf{C}\mathbf{x}_l$ are the elements of the damping matrix in modal co-ordinates. For the case $k = j$, neglecting the second order terms involving $\alpha_l^{(j)}$ and C'_{kl}, $\forall k \neq l$, equation (7) yields

$$-\lambda_j^2 + \mathrm{i}\lambda_j C'_{jj} + \omega_j^2 \approx 0,$$

or

$$\lambda_j \approx \pm\, \omega_j + \mathrm{i}C'_{jj}/2, \tag{8}$$

which is the approximate expression for the complex natural frequencies. For the case $k \neq j$ in (7), again retaining only the first order terms, gives

$$\alpha_k^{(j)} \approx \frac{\mathrm{i}\omega_j C'_{kj}}{(\omega_j^2 - \omega_k^2)}. \tag{9}$$

Thus, from the assumed expansion (6) the first order approximate expression of the complex eigenvectors is

$$\mathbf{z}_j \approx \mathbf{x}_j + \mathrm{i} \sum_{\substack{k=1 \\ k \neq j}}^{N} \frac{\omega_j C'_{kj}}{(\omega_j^2 - \omega_k^2)} \mathbf{x}_k. \tag{10}$$

These results were obtained by Rayleigh [2, see section 102, equations (5) and (6)]. The above equation shows (up to first order approximation) that the real parts of the complex modes are the same as the undamped modes and that the off-diagonal terms of the modal damping matrix are responsible for the imaginary parts.

3. IDENTIFICATION OF THE VISCOUS DAMPING MATRIX

Most of the common methods for experimental determination of the damping parameters use the proportional damping assumption. A typical procedure can be described as follows:

1. Measure a set of transfer functions $H_{ij}(\omega)$ at a set of grid points on the structure.
2. Obtain the natural frequencies ω_k by a pole-fitting method.
3. Evaluate the modal half-power bandwidth $\Delta\omega_k$ from the frequency response functions, then the Q-factor $Q_k = \omega_k/\Delta\omega_k$ and the modal damping factor $\zeta_k = 1/2Q_k$.
4. Determine the modal amplitude factors a_k to obtain the mode shapes, $\mathbf{z}_k$.
5. Finally, reconstruct some transfer functions to verify the accuracy of the evaluated parameters.

Such a procedure does not provide reliable information about the nature or spatial distribution of the damping, though the reconstructed transfer functions may match the measured ones well.

The next stage, followed by many researchers, is to attempt to obtain the full viscous damping matrix from the experimental measurements. Methods can be divided into two basic categories: (a) damping identification from modal testing and analysis [14–17] and (b) direct damping identification from the forced response measurements [18, 4, 19]. All these methods are based on the assumption that the damping mechanism of the structure is viscous, and their efficacy when the damping mechanism is not viscous is largely unexplored. Here a method is proposed to obtain the full non-proportional viscous damping matrix from complex modal data, in a way which will generalize very naturally to the fitting of non-viscous damping models in the companion paper [9]. The perturbation expression from the previous section is used as the basis of the fitting procedure, and it is assumed that the damping is sufficiently light to justify this.

Approximate complex natural frequencies and mode shapes for a system with light viscous damping can be obtained from the expressions given in equations (8) and (10). Write

$$\hat{\mathbf{z}}_j = \hat{\mathbf{u}}_j + \mathrm{i}\hat{\mathbf{v}}_j, \tag{11}$$

where $\hat{\mathbf{z}}_j \in \mathbb{C}^N$ is the measured jth complex mode, and $\hat{\mathbf{u}}_j$, $\hat{\mathbf{v}}_j$ are both real. Suppose that the number of modes to be considered in the study is m: in general $m \neq N$, usually $N \geqslant m$. If the measured complex mode shapes are consistent with a viscous damping model then from equation (8) the real part of each complex natural frequency gives the undamped natural frequency:

$$\hat{\omega}_j = \Re(\hat{\lambda}_j), \tag{12}$$

where $\hat{\lambda}_j$ denotes the jth complex natural frequency measured from the experiment. Similarly, from equation (10), the real part of each complex mode $\hat{\mathbf{u}}_j$ immediately gives the corresponding undamped mode and the mass orthogonality relationship (5) will be automatically satisfied. Now, from equation (10), expand the imaginary part of $\hat{\mathbf{z}}_j$ as a linear combination of $\hat{\mathbf{u}}_j$:

$$\hat{\mathbf{v}}_j = \sum_{k=1}^{m} B_{kj}\hat{\mathbf{u}}_k \quad \text{where } B_{kj}(\hat{\omega}_j^2 - \hat{\omega}_k^2) = \hat{\omega}_j C'_{kj}. \tag{13}$$

With $N \geqslant m$ this relation cannot be satisfied exactly in general. Then the constants B_{kj} should be calculated such that the error in representing $\hat{\mathbf{v}}_j$ by such a sum is minimized. Note that in the above sum the $k = j$ term has been included although in the original sum in equation (10) this term was absent. This is done to simplify the mathematical formulation to be followed, and has no effect on the result. The interest lies in calculating C'_{kj} from B_{kj} through the relationship given by the second part of equation (13), and indeed when $k = j$ then $C'_{kj} = 0$. The diagonal terms C'_{jj} are instead obtained from the imaginary part of the complex natural frequencies

$$C'_{jj} = 2\Im(\hat{\lambda}_j). \tag{14}$$

The error from representing $\hat{\mathbf{v}}_j$ by the series sum (13) can be expressed as

$$\varepsilon_j = \hat{\mathbf{v}}_j - \sum_{k=1}^{m} B_{kj}\hat{\mathbf{u}}_k. \tag{15}$$

To minimize the error a Galerkin approach can be adopted. The undamped mode shapes $\hat{\mathbf{u}}_l$, $l = 1, \ldots, m$, are taken as "weighting functions". Using the Galerkin method on $\varepsilon_j \in \mathbb{R}^N$ for a fixed j one obtains

$$\hat{\mathbf{u}}_l^{\mathrm{T}}\varepsilon_j = 0, \quad l = 1, \ldots, m. \tag{16}$$

Combining equations (15) and (16) yields

$$\hat{\mathbf{u}}_l^{\mathrm{T}}\left\{\hat{\mathbf{v}}_j - \sum_{k=1}^{m} B_{kj}\hat{\mathbf{u}}_k\right\} = 0 \quad \text{or} \quad \sum_{k=1}^{m} W_{lk}B_{kj} = S_{lj}, \ l = 1, \ldots, m \tag{17}$$

with $W_{lk} = \hat{\mathbf{u}}_l^{\mathrm{T}}\hat{\mathbf{u}}_k$ and $S_{lj} = \hat{\mathbf{u}}_l^{\mathrm{T}}\hat{\mathbf{v}}_j$. Since W_{kl} is j-independent, for all $j = 1, \ldots, m$ the above equations can be combined in matrix form

$$\mathbf{WB} = \mathbf{S}, \tag{18}$$

where $\mathbf{B} \in \mathbb{R}^{m\times m}$ is the matrix of unknown coefficients to be found, $\mathbf{W} = \hat{\mathbf{U}}^{\mathrm{T}}\hat{\mathbf{U}} \in \mathbb{R}^{m\times m}$ and $\mathbf{S} = \hat{\mathbf{U}}^{\mathrm{T}}\hat{\mathbf{V}} \in \mathbb{R}^{m\times m}$ with

$$\hat{\mathbf{U}} = [\hat{\mathbf{u}}_1, \hat{\mathbf{u}}_2, \ldots, \hat{\mathbf{u}}_m] \in \mathbb{R}^{N\times m}, \quad \hat{\mathbf{V}} = [\mathbf{v}_1, \hat{\mathbf{v}}_2, \ldots, \hat{\mathbf{v}}_m] \in \mathbb{R}^{N\times m}. \tag{19}$$

Now, $\mathbf{B}$ can be obtained by carrying out the matrix inversion associated with equation (18) as

$$\mathbf{B} = \mathbf{W}^{-1}\mathbf{S} = [\hat{\mathbf{U}}^{\mathrm{T}}\hat{\mathbf{U}}]^{-1}\hat{\mathbf{U}}^{\mathrm{T}}\mathbf{V}. \tag{20}$$

From the **B** matrix, the coefficients of the modal damping matrix can be derived from

$$C'_{kj} = \frac{(\hat{\omega}_j^2 - \hat{\omega}_k^2)B_{kj}}{\hat{\omega}_j}, \quad k \neq j. \tag{21}$$

The above two equations together with equation (14) completely define the modal damping matrix $\mathbf{C}' \in \mathbb{R}^{m \times m}$. If $\hat{\mathbf{U}} \in \mathbb{R}^{N \times N}$ is the *complete* undamped modal matrix then the damping matrices in the modal co-ordinates and original co-ordinates are related by $\mathbf{C}' = \hat{\mathbf{U}}^{\mathrm{T}}\mathbf{C}\hat{\mathbf{U}}$. Thus given $\mathbf{C}'$, the damping matrix in the original co-ordinates can be easily obtained by the inverse transformation as $\mathbf{C} = \mathbf{U}^{\mathrm{T}^{-1}}\mathbf{C}'\mathbf{U}^{-1}$. For the case when the full modal matrix is not available, that is $\hat{\mathbf{U}} \in \mathbb{R}^{N \times m}$ is not a square matrix, a pseudoinverse is required in order to obtain the damping matrix in the original co-ordinates. The damping matrix in the original co-ordinates is then given by

$$\mathbf{C} = [(\hat{\mathbf{U}}^{\mathrm{T}}\hat{\mathbf{U}})^{-1}\hat{\mathbf{U}}^{\mathrm{T}}]^{T}\mathbf{C}'[(\mathbf{U}^{\mathrm{T}}\hat{\mathbf{U}})^{-1}\mathbf{U}^{\mathrm{T}}]. \tag{22}$$

It is clear from the above equations that only the complex natural frequencies and mode shapes are needed to obtain **C**. The method is very simple and does not require much computational time. Another advantage is that neither the estimation of mass and stiffness matrices nor the full set of modal data is required to obtain an estimate of the full damping matrix. Using a larger number of modes will of course produce better results with higher spatial resolution. In summary, this procedure can be described by the following steps:

1. Measure a set of transfer functions $H_{ij}(\omega)$.
2. Choose the number m of modes to be retained in the study. Determine the complex natural frequencies $\hat{\lambda}_j$ and complex mode shapes $\hat{\mathbf{z}}_j$ from the transfer functions, for all $j = 1, \ldots, m$. Obtain the complex mode shape matrix $\hat{\mathbf{Z}} = [\hat{\mathbf{z}}_1, \hat{\mathbf{z}}_2, \ldots, \mathbf{z}_m] \in \mathbb{C}^{N \times m}$.
3. Estimate the "undamped natural frequencies" as $\hat{\omega}_j = \Re(\hat{\lambda}_j)$.
4. Set $\hat{\mathbf{U}} = \Re[\hat{\mathbf{Z}}]$ and $\hat{\mathbf{V}} = \Im[\hat{\mathbf{Z}}]$, and from these obtain $\mathbf{W} = \hat{\mathbf{U}}^{\mathrm{T}}\hat{\mathbf{U}}$ and $\mathbf{S} = \hat{\mathbf{U}}^{\mathrm{T}}\hat{\mathbf{V}}$. Now denote $\mathbf{B} = \mathbf{W}^{-1}\mathbf{S}$.
5. From the **B** matrix get $C'_{kj} = (\hat{\omega}_j^2 - \hat{\omega}_k^2)B_{kj}/\hat{\omega}_j$ for $k \neq j$ and $C'_{jj} = 2\Im(\hat{\lambda}_j)$.
6. Finally, carry out the transformation $\mathbf{C} = [(\hat{\mathbf{U}}^{\mathrm{T}}\mathbf{U})^{-1}\hat{\mathbf{U}}^{\mathrm{T}}]^{\mathrm{T}}\mathbf{C}'[(\hat{\mathbf{U}}^{\mathrm{T}}\hat{\mathbf{U}})^{-1}\hat{\mathbf{U}}^{\mathrm{T}}]$ to get the damping matrix in physical coordinates.

It should be observed that even if the measured transfer functions are reciprocal, this procedure does not necessarily yield a symmetric damping matrix. If indeed a non-symmetric damping matrix is obtained then it may be deduced that the physical law behind the damping mechanism in the structure is not viscous. This fact is illustrated by example in the next section. Under those circumstances, if an accurate model for the damping in the structure is needed then a non-viscous model of some kind must be fitted to the measured data. Some examples of such models and algorithms for fitting them will be illustrated in the companion paper [9].

4. NUMERICAL EXAMPLES

There is a major difference in emphasis between this study and other related studies on damping identification reported in the literature. Most of the methods assume from the outset that the system is viscously damped (see the review paper by Pilkey and Inman [20]) and then formulate the theory to identify a viscous damping matrix. Here, it is intended to investigate how much can be learnt by fitting a viscous damping model when the actual system is non-viscously damped, as must be expected to be the case for most practical

systems. It is far from clear in practice what kind of non-viscous damping behaviour a system might exhibit. That question is deferred for the moment, and instead a system which has a known non-viscous damping model is studied by simulation. Two different physically realistic non-viscous damping models are considered in this study. They are applied to a system consisting of a linear array of spring-mass oscillators and dampers.

This simple system provides a useful basis to carry out numerical investigations. Complex natural frequencies and modes can be calculated for the model system using the procedure outlined by Woodhouse [6], then treated like experimental data obtained from a modal-testing procedure, and used for identifying a viscous damping model by the procedure described in the previous section. Note that in a true experimental environment the measured complex natural frequencies and mode shapes will be contaminated by noise. Since the simulation data are noise-free, the results obtained using them are "ideal", the best that can be hoped for using this approach. Once promising algorithms have been identified in this way, the influence of noise in degrading the performance will have to be addressed.

Figure 1 shows the model systems. N masses, each of mass m_u, are connected by springs of stiffness k_u. The mass matrix of the system has the form $\mathbf{M} = m_u \mathbf{I}_N$, where $\mathbf{I}_N$ is the $N \times N$ identity matrix. The stiffness matrix of the system is

$$\mathbf{K} = k_u \begin{bmatrix} 2 & -1 & & & & & \\ -1 & 2 & -1 & & & & \\ & \ddots & \ddots & \ddots & & & \\ & & -1 & 2 & -1 & & \\ & & & \ddots & \ddots & & \\ & & & & & -1 & 2 \end{bmatrix}. \tag{23}$$

Certain of the masses of the system shown in Figure 1(a) have dissipative elements connecting them to the ground. In this case, the damping force depends only on the absolute motion of the individual masses. Such damping will be described as "locally reacting" by analogy with usage in the theory of fluid-loaded structures (see, e.g., Crighton [21]). For the system shown in Figure 1(b), by contrast, dissipative elements are connected between certain adjacent pairs of masses. In this case, the damping force depends on the relative motion of the two adjacent masses, and will be called "non-locally reacting".

The dissipative elements shown in Figure 1 will be taken to be linear, but not to be simple viscous dashpots. For any such element, the force developed between the two ends will depend on the history of the relative motion of the two ends. The dependence can be written

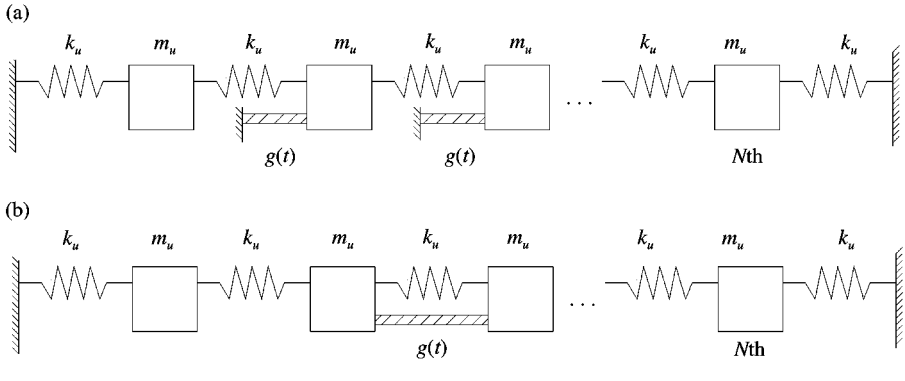

Figure 1. Linear array of N spring–mass oscillators, $N = 30$, $m_u = 1$ Kg, $k_u = 4 \times 10^3$ N/m.

in terms of a convolution integral. Using the mass and the stiffness matrices described before, the equations of motion can thus be expressed in the form

$$\mathbf{M}\ddot{\mathbf{y}}(t) + \bar{\mathbf{C}}\int_{-\infty}^{t} g(t-\tau)\dot{\mathbf{y}}(\tau)\,\mathrm{d}\tau + \mathbf{K}\mathbf{y}(t) = \mathbf{0}, \tag{24}$$

where $g(t)$ is the damping function (assumed to have the same form for all the damping elements in the system) and $\bar{\mathbf{C}}$ is the associated coefficient matrix which depends on the distribution of the dampers. Two specific damping models will be considered, defined by two different forms of $g(t)$:

- MODEL 1 (exponential):

$$g^{(1)}(t) = \mu_1 \mathrm{e}^{-\mu_1 t}, \quad t \geqslant 0, \tag{25}$$

- MODEL 2 (Gaussian):

$$g^{(2)}(t) = 2\sqrt{\frac{\mu_2}{\pi}}\mathrm{e}^{-\mu_2 t^2}, \quad t \geqslant 0, \tag{26}$$

where μ_1 and μ_2 are constants. Any physically realistic damping model must satisfy a condition of positive energy dissipation at all frequencies. A sufficient condition to guarantee this, satisfied by both models considered here, is described in the companion paper [9].

It is convenient to normalize the functions to make comparisons between models meaningful. Both functions have already been scaled so as to have unit area when integrated to infinity. This makes them directly comparable with the viscous model, in which the corresponding damping function would be a unit delta function, $g(t) = \delta(t)$, and the coefficient matrix $\bar{\mathbf{C}}$ would be the usual damping matrix. It is also convenient to define a characteristic time constant θ_j for each damping function, via the first moment of $g^{(j)}(t)$:

$$\theta_j = \int_0^{\infty} t g^{(j)}(t)\,\mathrm{d}t. \tag{27}$$

For the two damping models considered here, evaluating the above integral gives $\theta_1 = 1/\mu_1$ and $\theta_2 = 1/\sqrt{\pi\mu_2}$. For viscous damping $\theta_j = 0$. The characteristic time constant of a damping function gives a convenient measure of "width": if it is close to zero the damping behaviour will be near-viscous, and *vice versa*. To establish an equivalence between the two damping models they can be chosen to have the same time constant, so that $1/\mu_1 = 1/\sqrt{\pi\mu_2}$.

For the system with locally reacting damping shown in Figure 1(a), $\bar{\mathbf{C}} = c\bar{\mathbf{I}}$, where c is a constant and $\bar{\mathbf{I}}$ is a block identity matrix which is non-zero only between the s-th and $(s + l)$th entries along the diagonal, so that s denotes the first damped mass and $(s + l)$ the last one. For the system with non-locally reacting damping shown in Figure 1(b), $\bar{\mathbf{C}}$ has a similar pattern to the stiffness matrix given by equation (23), but non-zero only for terms relating to the block between s and $(s + l)$. For the numerical calculations considered here, $N = 30$, $s = 8$ and $(s + l) = 17$.

For the purpose of numerical examples, the values $m_u = 1$ kg, $k_u = 4 \times 10^5$ N/m have been used. The resulting undamped natural frequencies then range from near zero to approximately 200 Hz. For damping models, the value $c = 25$ has been used, and various values of the time constant θ have been tested. These are conveniently expressed as

a fraction of the period of the highest undamped natural frequency:

$$\theta = \gamma T_{min}. \tag{28}$$

When γ is small compared with unity the damping behaviour can be expected to be essentially viscous, but when γ is of order unity non-viscous effects should become significant.

The complex natural frequencies and mode shapes can now be calculated from the first order perturbation expression given by Woodhouse [6] (also see section 2 of the companion paper [9]). The steps outlined in the previous section can then be followed to obtain an equivalent viscous damping which represents these "measured" data most accurately.

4.1. RESULTS FOR SMALL γ

When $\gamma = 0{\cdot}02$ both damping models should show near-viscous behaviour. First, consider the system shown in Figure 1(a) with locally reacting damping. Figure 2 shows the fitted viscous damping matrix **C** for damping model 2, calculated using the complete set of 30 modes. The fitted matrix identifies the damping in the system very well. The high portion of the plot corresponds to the spatial location of the dampers. The off-diagonal terms of the identified damping matrix are very small compared to the diagonal terms, indicating correctly that the damping is locally reacting.

It is useful to understand the effect of modal truncation on the damping identification procedure. In practice, it might be expected to be able to use only the first few modes of the system to identify the damping matrix. Figures 3 and 4 show the fitted viscous damping matrix using, respectively, the first 20 and the first 10 modes only. The quality of the fitted damping matrix gradually deteriorates as the number of modes used to fit the damping matrix is reduced, but still the identified damping matrix shows a reasonable approximation to the true behaviour. The spatial resolution of the identified damping is limited by that of the set of modes used, and some off-diagonal activity is seen in the fitted matrix. Since for this system the mode shapes are approximately sinusoidal, the effects of modal truncation can be recognized as analogous to Gibbs' phenomenon in a truncated Fourier series.

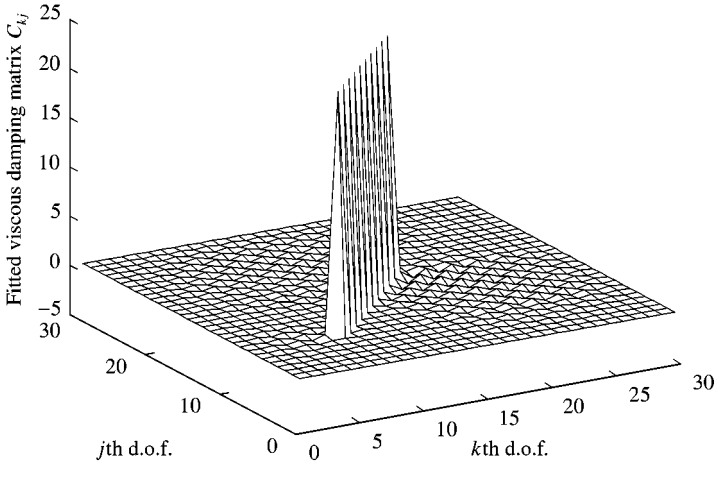

Figure 2. Fitted viscous damping matrix for the local case, $\gamma = 0{\cdot}02$, damping model 2.

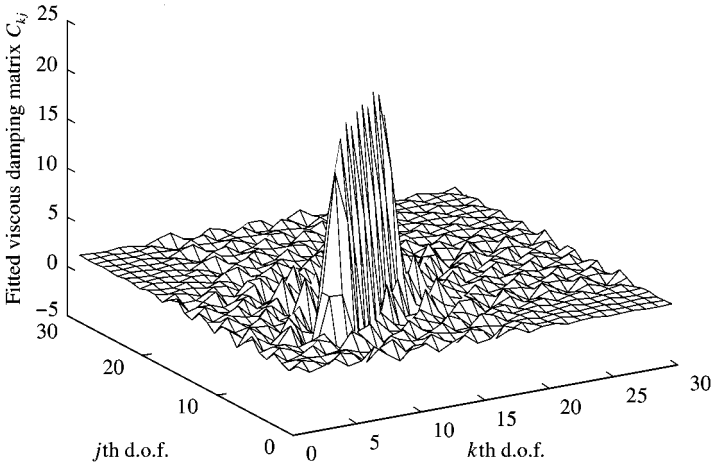

Figure 3. Fitted viscous damping matrix using first 20 modes for the local case, $\gamma = 0{\cdot}02$, damping model 2.

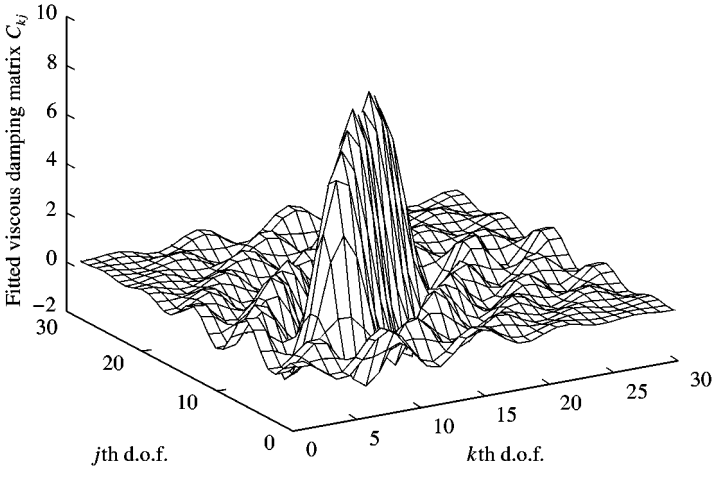

Figure 4. Fitted viscous damping matrix using first 10 modes for the local case, $\gamma = 0{\cdot}02$, damping model 2.

Now, consider the system shown in Figure 1(b) with non-locally reacting damping. Figure 5 shows the fitted viscous damping matrix for damping model 2, using the full set of modes. Again, the fitted matrix identifies the damping in the system quite well. The high portion of the plot corresponds to the spatial location of the dampers. The negative off-diagonal terms in the identified damping matrix indicate that the damping is non-locally reacting, and the pattern is recognizably that of equation (23). The extent of noise away from the three diagonals is rather higher than was the case in Figure 2. This is not very surprising. The pattern of terms along a row of the matrix corresponding to a damped position was, in the former case, a discrete approximation to a delta function. In the latter case it is an approximation to the second derivative of a delta function. The modal expansion, approximately a Fourier series, will thus have a much larger contribution from the higher modes, which are the first to be affected by the non-zero width of the damping function. A higher level of noise is the inevitable result.

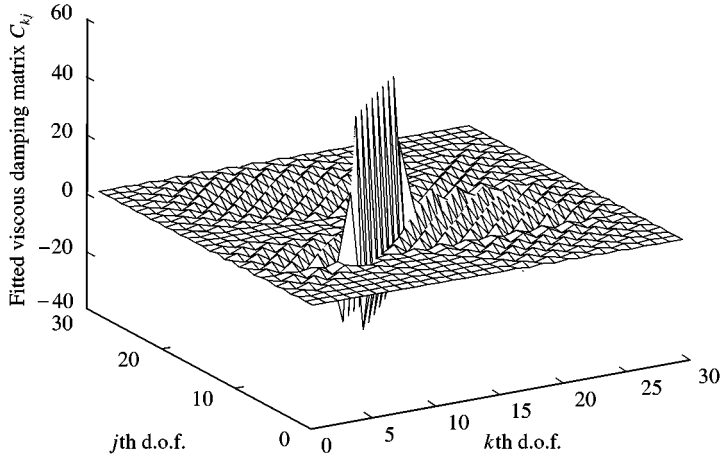

Figure 5. Fitted viscous damping matrix for the non-local case, $\gamma = 0{\cdot}02$, damping model 2.

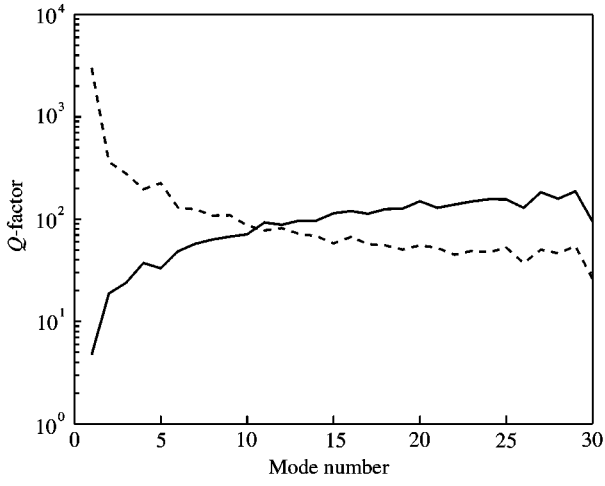

Figure 6. Modal Q-factors, $\gamma = 0{\cdot}02$, damping model 2; (——), locally reacting damping; (– – –), non-locally reacting damping.

One consequence of the distinction between local and non-local damping is illustrated in Figure 6. The modal Q-factors are plotted for the two cases studied, for the full set of 30 modes. Locally reacting damping (solid line) produces a Q-factor roughly proportional to mode number. The particular non-local damping chosen here shows the opposite trend, with Q-factors roughly inversely proportional to mode number (dashed line). Both trends can be understood in terms of Rayleigh damping. If the damping extended over the entire structure rather that being limited to a finite patch, then the local-reacting damping would correspond to a dissipation matrix proportional to the mass matrix, while the non-local damping would correspond to a dissipation matrix proportional to the stiffness matrix. The trends of modal Q-factor with frequency would then be exactly proportional and inversely proportional respectively. Limiting the damping to a part of the structure has evidently not disturbed this pattern very much. The variation with frequency has translated into

a variation with mode number: the mode number relates rather directly to wavenumber for this simple system, and the physical origins of the different trends of Q-factors are dependent on wavelength, rather than on frequency as such.

When the fitting procedure is repeated using the alternative damping model of equation (25) the results are sufficiently similar and are not reproduced here. Since the time constant is so short, both damping models are near to viscous damping and the detailed difference in their functional behaviour does not influence the results significantly. In summary, it can be said that when the time constant for a damping model is small the proposed identification method works quite well regardless of the functional form of the damping mechanism. The spatial location of damping is revealed clearly, and also whether it is locally or non-locally reacting. Modal truncation blurs the results, but does not invalidate the identification process.

4.2. RESULTS FOR LARGER γ

When γ is larger the two non-viscous damping models depart from the viscous damping model, each in its own way. For the value $\gamma = 0{\cdot}5$, Figure 7(a) shows the result of running the fitting procedure for damping model 1 (equation (25)) with locally reacting damping and the full set of modes, similar to Figure 2. Figure 7(b) shows the corresponding fitted viscous damping matrix $\mathbf{C}$ for damping model 2 (equation (26)). In both cases it may be noted that although we have started with a locally reacting damping model, which means the matrix is non-zero only along the diagonal, the non-zero values in the off-diagonal terms show that the fitted viscous damping is, in a sense, not locally reacting. Nevertheless, the spatial distribution of the damping is well identified, and perhaps one might be able to guess that the underlying mechanism was locally reacting from the fact that the significantly non-zero elements all have positive values, with a clear peak centered on the diagonal of the matrix. This remark remains true even for larger values of γ. Just one example is given: Figure 8 shows the fitted dissipation matrix for $\gamma = 2$. Most of the matrix elements are now significantly non-zero, but the pattern shows the same general features as Figure 7(a). The high values, along the main diagonal of the matrix, still correctly identify the spatial distribution of the damping.

Figures 9(a) and 9(b) show the fitted results corresponding to Figures 7(a) and 7(b), using the non-local damping model. Similar remarks can be made as for the locally reacting case. The spatial distribution of the damping is revealed quite clearly and correctly. The non-local nature of the damping is hinted at by the strong negative values on either side of the main diagonal of the matrix. In both cases, there is an obvious echo of the pattern seen in Figure 5 and equation (23).

To give a different insight into the behaviour of the various damping models it is useful to see the pattern of modal damping factors. In Figure 10, the modal Q-factors are plotted for the two damping models with $\gamma = 0{\cdot}5$, in the local-reacting case. Figure 11 shows the corresponding results for the non-locally reacting case. For locally reacting damping the Q-factors rise with mode number, for both damping models. For the non-local case the Q-factors fall initially. For damping model 1 and these particular parameter values the Q-factors are then approximately constant, while for damping mode 2 they rise again after a while, reaching very high values at high mode numbers. In terms of physical plausibility, damping model 1 in the non-local configuration gives the closest match to the common practical experience that modal damping factors are approximately constant. However, physical plausibility is not a major issue here, where the aim is to test the procedure under a wide range of circumstances.

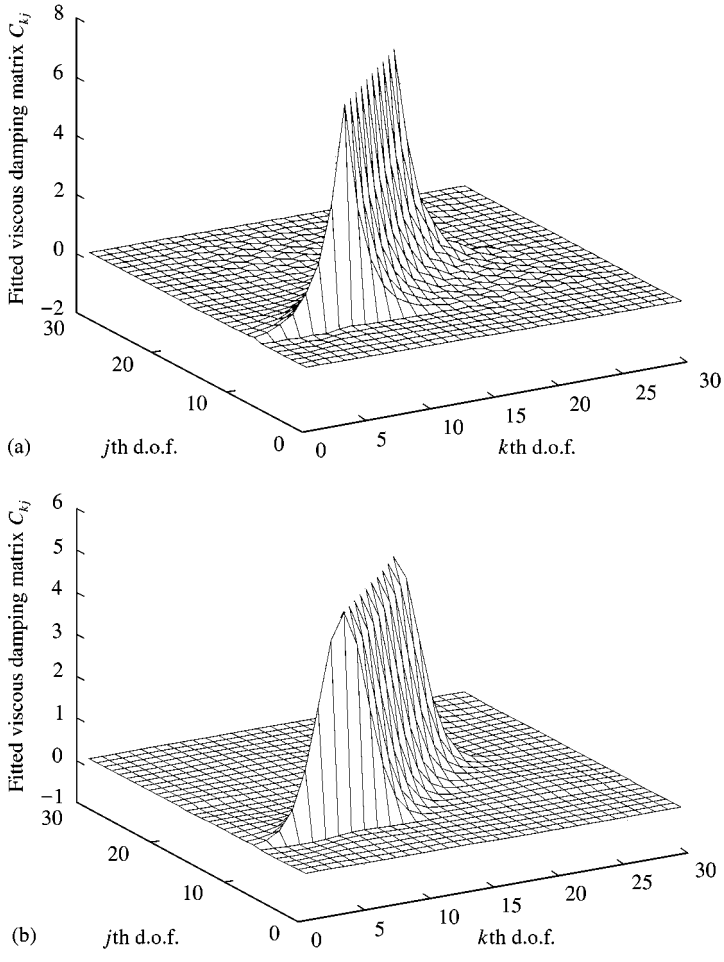

Figure 7. (a) Fitted viscous damping matrix for the local case, $\gamma = 0{\cdot}5$, damping model 1. (b) Fitted viscous damping matrix for the local case, $\gamma = 0{\cdot}5$, damping model 2.

To judge the numerical accuracy of the fitted viscous damping it is useful to reconstruct transfer functions. It is easy to do this, by inverting the dynamic stiffness matrix using the fitted viscous damping matrix. A typical transfer function $H_{kj}(\omega)$, for $k = 11$ and $j = 24$ is shown in Figure 12, based on locally reacting damping using damping model 1. It is clear that the reconstructed transfer function agrees well with the original one. This is to be expected: the fitting procedure outlined in the previous section is exact, within the approximations of the small-damping perturbation theory, provided that the full set of modes is used. The full set of poles and their residues are correctly reproduced—this is the essential contrast between this approach and one which fits only proportional damping, for which the poles can be correct but the residues cannot (because they will be real, not complex). This result has a far-reaching implication: an incorrect damping model (the fitted viscous damping) with a different spatial distribution from the true locally reacting model can reproduce accurately the full set of transfer functions. This means that by measuring transfer functions it is not possible to identify uniquely the governing mechanism.

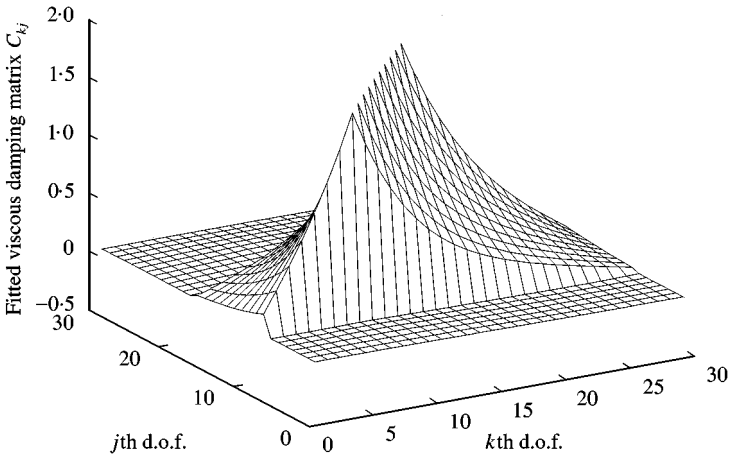

Figure 8. Fitted viscous damping matrix for the local case, $\gamma = 2{\cdot}0$, damping model 1.

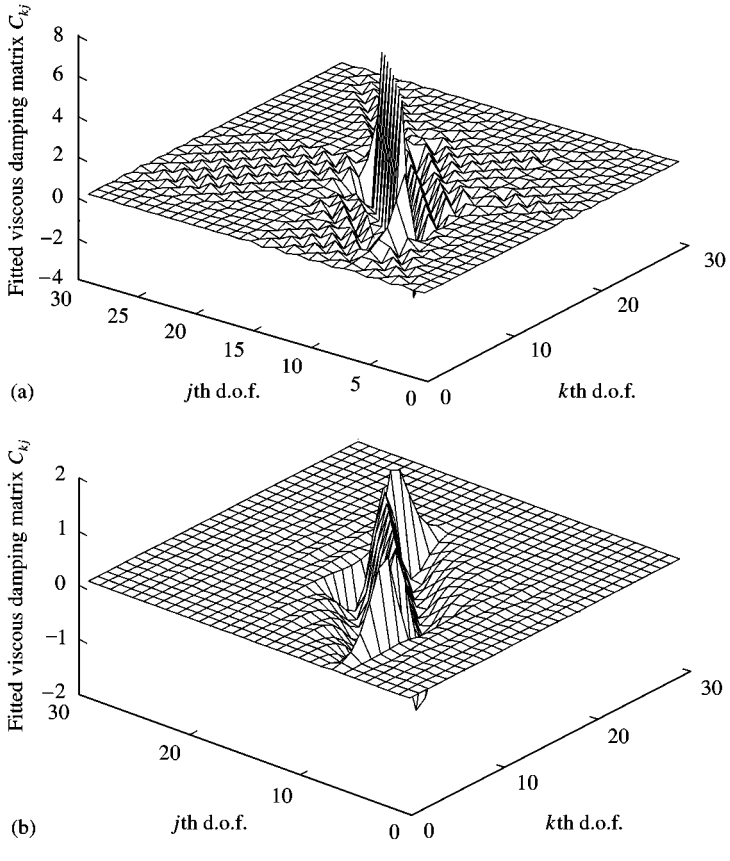

Figure 9. (a) Fitted viscous damping matrix for the non-local case, $\gamma = 0{\cdot}5$, damping model 1. (b) Fitted viscous damping matrix for the non-local case, $\gamma = 0{\cdot}5$, damping model 2.

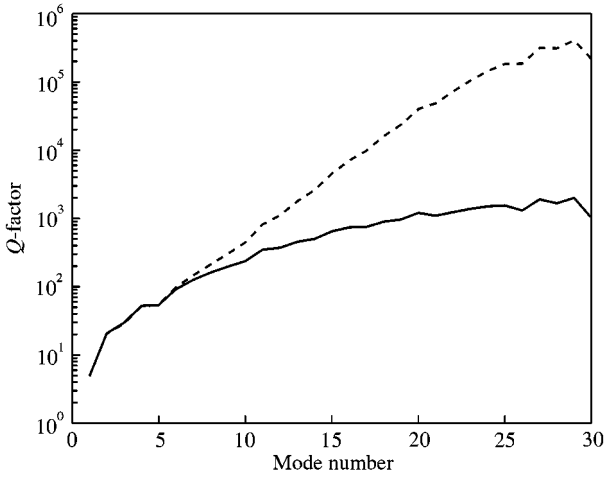

Figure 10. Modal Q-factors for the local case, $\gamma = 0{\cdot}5$; (——), model 1; (– – –), model 2.

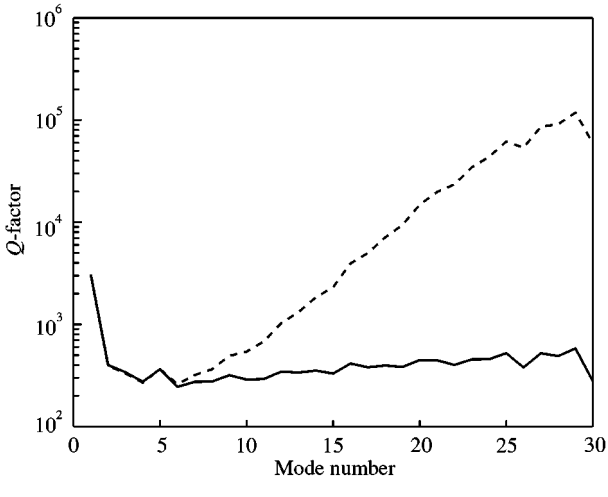

Figure 11. Modal Q-factors for the non-local case, $\gamma = 0{\cdot}5$; (——), model 1; (– – –), model 2.

However, it should be noted that in all cases of Figures 7(a)–9(b) the fitted damping matrix is not symmetric. This is, in some sense, a non-physical result. In view of this non-symmetry, it is interesting to check the reciprocity of the transfer functions. In Figure 12, the reciprocal transfer function $H_{jk}(\omega)$ is also plotted, as a dashed line. It is not visible as a separate line in the figure, because it matches $H_{kj}(\omega)$ with good accuracy. This plot demonstrates that the non-symmetry of the fitted viscous damping in the spatial co-ordinate does not necessarily affect the reciprocity of the transfer functions. Instead, non-symmetry of a fitted dissipation matrix should be regarded as evidence that the true damping model is not viscous. To obtain a correct physical description of the damping, a non-viscous model should be fitted instead. This idea is developed in the companion paper [9].

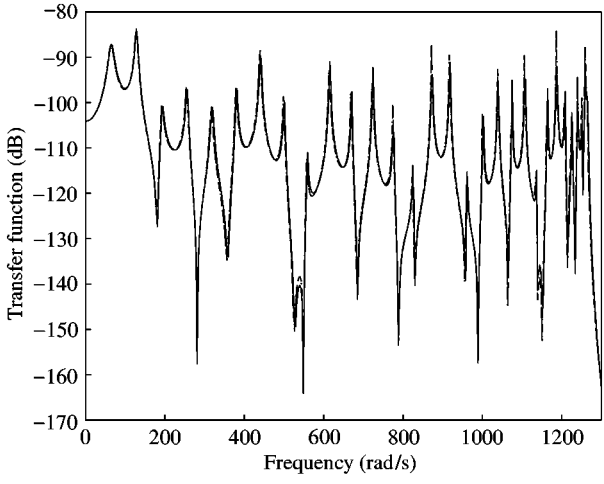

Figure 12. Transfer functions for the local case, $\gamma = 0{\cdot}5$, damping model 1, $k = 11$, $j = 24$; (——), exact $H_{kj}(\omega)$; (– – –), fitted $H_{kj}(\omega)$; (– — –), fitted $H_{jk}(\omega)$.

5. CONCLUSIONS

In this paper, a method has been proposed to identify a non-proportional viscous damping matrix in vibrating systems. It is assumed that damping is light so that the first order perturbation method is applicable. The method is simple, direct, and compatible with conventional modal testing procedures. The complex modes and natural frequencies are used, but the method does not require either the full set of modal data, nor any knowledge of the mass and stiffness matrices. The validity of the proposed method has been explored by applying it to simulated data from a simple test problem, in which a linear array of spring-mass oscillators is damped by non-viscous elements over part of its length.

Numerical experiments have been carried out with a wide range of parameter values and different damping models. The main features of the results have been illustrated by two particular damping models and representative parameter values. It has been shown that the method generally predicts the spatial location of the damping with good accuracy, and also gives a good indication of whether the damping is locally reacting or not. Whatever be the nature of the fitted damping matrix, the transfer functions obtained from the fitted viscous damping agree well with the exact transfer functions of the simulated system. Reciprocity of the transfer functions remains preserved within an acceptable accuracy although in some cases the fitted viscous damping is not symmetric.

Symmetry breaking of the fitted viscous damping matrix depends on the value of the characteristic time constant θ of the damping model, defined by equation (27). When θ is short compared with the natural periods of the vibration, the damping is effectively viscous and the fitting procedure gives a physically sensible symmetric matrix. When θ is larger, though, the memory of the damping function influences the detailed behaviour. Although the poles and residues of the transfer functions can still be fitted accurately with a model of viscous form, the underlying non-viscous behaviour manifests itself in a non-symmetrical matrix. If a correct physical description of the damping mechanism is needed, then a suitable non-viscous model must be selected and fitted. This question is taken up in the companion paper [9].

ACKNOWLEDGMENTS

The first author is grateful to the Nehru Memorial Trust, London and Cambridge Commonwealth Trust for providing financial support for this research.

REFERENCES

1. LORD RAYLEIGH 1877 *Theory of Sound* (*two volumes*). New York: Dover Publications, 1945 re-issue, second edition.
2. A. SESTIERI and R. IBRAHIM 1994 *Journal of Sound and Vibration* **177**, 145–157. Analysis of errors and approximations in the use of modal coordinates.
3. S. R. IBRAHIM 1983 *American Institute of Aeronautics and Astronautics Journal* **21**, 446–451. Computation of normal modes from identified complex modes.
4. S. Y. CHEN, M. S. JU and Y. G. TSUEI 1996 *Mechanical System and Signal Processing* **10**, 93–106. Extraction of normal modes for highly coupled incomplete systems with general damping.
5. E. BALMÈS 1997 *Mechanical System and Signal Processing* **11**, 229–243. New results on the identification of normal modes from experimental complex modes.
6. J. WOODHOUSE 1998 *Journal of Sound and Vibration* **215**, 547–569. Linear damping models for structural vibration.
7. D. J. EWINS 1984 *Modal Testing*: *Theory and Practice*. Taunton: Research Studies Press.
8. Y. C. FUNG 1965 *Foundations of Solid Mechanics*. Englewood Cliffs, NJ: Prentice-Hall Inc.
9. S. ADHIKARI and J. WOODHOUSE 2000 *Journal of Sound and Vibration* **243**, 63–88. Identification of damping: Part 2, non-viscous damping.
10. P. LANCASTER 1966 *Lambda-matrices and Vibrating System* London: Pergamon Press.
11. T. K. CAUGHEY and M. E. J. O'KELLY 1965 *American Society of Mechanical Engineers Journal of Applied Mechanics* **32**, 583–588. Classical normal modes in damped linear dynamic systems.
12. D. E. NEWLAND 1989 *Mechanical Vibration Analysis and Computation*. New York: Longman, Harlow and John Wiley.
13. D. L. CRONIN 1990 *Computer and Structures* **36**, 133–138. Eigenvalue and eigenvector determination of non-classically damped dynamic systems.
14. T. K. HASSELSMAN 1972 *American Institute of Aeronautics and Astronautics Journal* **10**, 526–527. A method of constructing a full modal damping matrix from experimental measurements.
15. S. R. IBRAHIM 1983 *American Institute of Aeronautics and Astronautics Journal* **21**, 898–901. Dynamic modelling of structures from measured complex modes.
16. C. MINAS and D. J. INMAN 1991 *American Society of Mechanical Engineers Journal of Vibration and Acoustics* **113**, 219–224. Identification of a nonproportional damping matrix from incomplete modal information.
17. K. F. ALVIN, L. D. PETERSON and K. C. PARK 1997 *American Institute of Aeronautics and Astronautics Journal* **35**, 1187–1194. Extraction of normal modes and full modal damping from complex modal parameters.
18. J. E. MOTTERSHEAD 1990 *American Institute of Aeronautics and Astronautics Journal* **28**, 559–561. Theory for the estimation of structural vibration parameters from incomplete data.
19. M. BARUCH 1997 *Technical Report TAE No*. 803 *Technion*, *Israel Faculty of Aerospace Engineering*, *Israel Institute of Technology*, *Haifa*. Identification of the damping matrix.
20. D. P. PILKEY and D. J. INMAN 1998 *Proceedings International Modal Analysis Conference—IMAC*, 104–110. Survey of damping matrix identification.
21. D. G. CRIGHTON 1985 *Proceedings of the Royal Society of London*, *Series A* **397**, 99–120. Acoustics of a stiff locally reacting structure.

APPENDIX A: NOMENCLATURE

$\mathbf{C}$	viscous damping matrix
$\mathbf{C}'$	viscous damping matrix in the modal coordinates
$\bar{\mathbf{C}}$	coefficient matrix associated with the non-viscous damping functions
$g^{(j)}(t)$	non-viscous damping functions
$H_{ij}(\omega)$	set of measured transfer functions
$\mathbf{K}$	stiffness matrix

$\mathbf{M}$	mass matrix
N	degrees-of-freedom of the system
m	number of measured modes
Q_j	Q-factor for the jth mode
t	time
T_{min}	minimum time period for the system
$\mathbf{x}_j$	jth undamped mode
$\mathbf{X}$	matrix containing $\mathbf{x}_j$
$\mathbf{y}(t)$	vector of generalized co-ordinates
$\mathbf{z}_j$	jth complex mode
$\hat{\mathbf{z}}_j$	jth measured complex mode
$\hat{\mathbf{U}}$	matrix containing $\hat{\mathbf{z}}_j$
$\hat{\mathbf{u}}_j$	real part of $\hat{\mathbf{z}}_j$
$\hat{\mathbf{U}}$	matrix containing $\hat{\mathbf{u}}_j$
$\hat{\mathbf{v}}_j$	imaginary part of $\hat{\mathbf{z}}_j$
$\hat{\mathbf{V}}$	matrix containing $\hat{\mathbf{v}}_j$
ω_j	jth undamped natural frequency
λ_j	jth complex natural frequency of the system
ε_j	error vector associated with the jth complex mode
$\alpha\}^{j)}$	constants associated with expansion of the jth elastic modes
ζ_j	jth modal damping factor
μ_1	constant associated with exponential damping function
μ_2	constant associated with Gaussian damping function
θ	characteristic time constant
γ	non-dimensional characteristic time constant
$\delta(t)$	Dirac delta function
$\mathbb{C}$	space of complex numbers
$\mathbb{R}$	space of real numbers
$\Re(\bullet)$	real part of $(\bullet)$
$\Im(\bullet)$	imaginary part of $(\bullet)$
$\hat{(\bullet)}$	estimated value of $(\bullet)$
$(\bullet)^{\mathrm{T}}$	matrix transpose of $(\bullet)$
$(\bullet)^{-1}$	matrix inverse of $(\bullet)$
$\dot{(\bullet)}$	derivative of $(\bullet)$ with respect to t